Mapping Equatorial Gullies on Mars

Liesbeth van Elswijk, L. Roelofs, S. J. Conway

Utrecht University
LPG

Abstract

Liesbeth van Elswijk
liesbeth331@gmail.com

1.1 Introduction

Gullies are common across the mid-latitudes on Mars [1-3], where *sublimation of seasonal CO_2 ice* drives their formation. Smaller, channelized features (Fig. 1) that share *morphological characteristics,* occur on slopes closer to the equator [4-6], where seasonal CO_2 frost is largely absent [7]. No study to date has systematically mapped or characterised these **equatorial gullies (EQG)** and their formation mechanism remains unresolved.

We present the first systematic study of equatorial gullies between **25°N and 25°S**, using HiRISE imagery and testing *candidate formation mechanisms* against their spatial distribution, morphology and topographic setting.

1.2 Objectives

(1) Map the **global distribution** and spatial clustering
(2) Characterise equatorial gully **morphology**
(3) Assess **topographic slope controls**

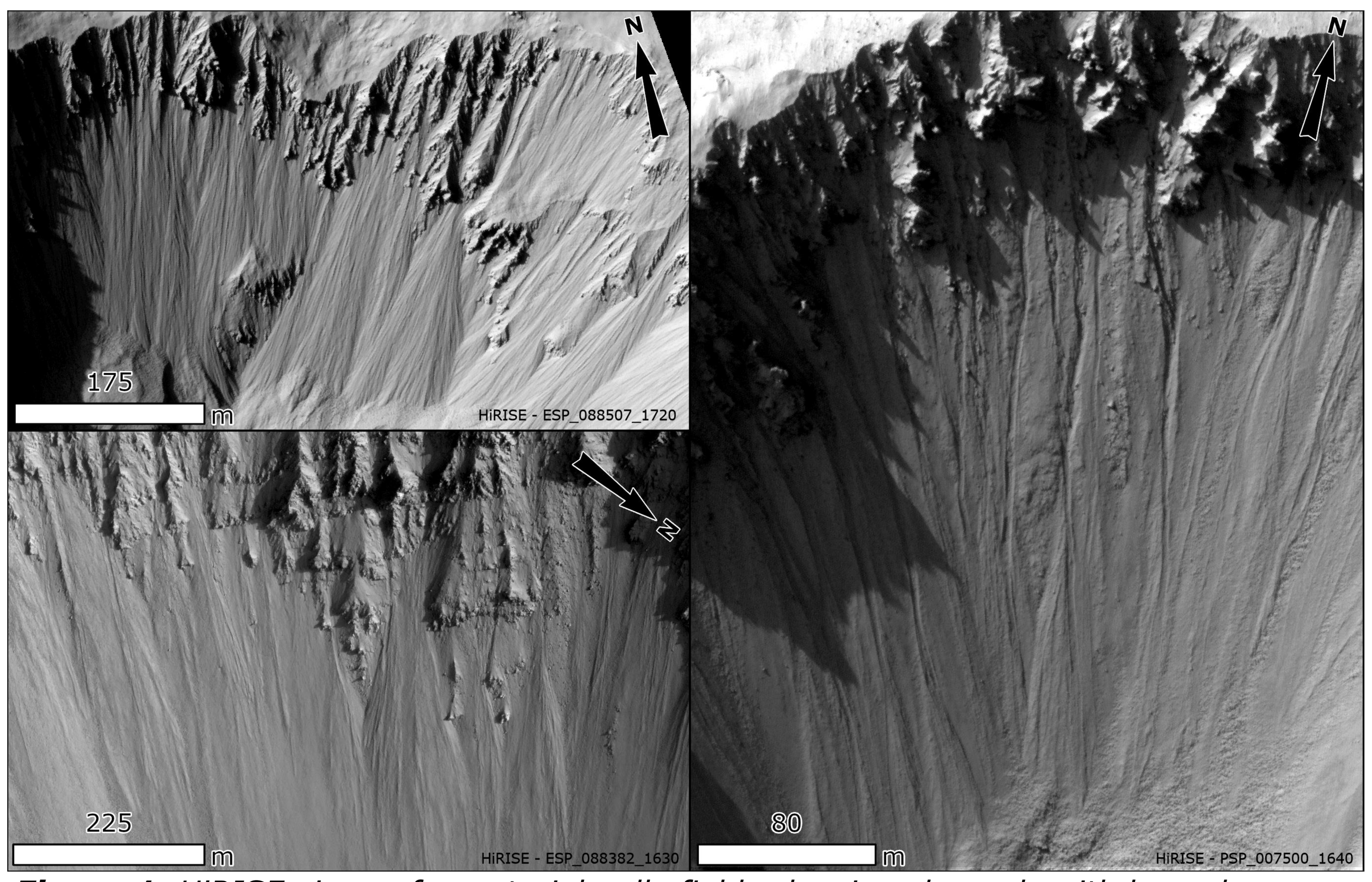

Figure 1. *HiRISE views of equatorial gully fields showing channels with leveed margins, extending from bedrock alcoves into depositional aprons with lobes.*

2. Methods

Mapping
HiRISE imagery, steep slopes >9°, y/n/m classification

Spatial and environmental analysis
Cluster analysis [8], Dust, Thermal Inertia, Elevation

Morphological mapping and analysis
481 gully fields, orientation, morphological expression

DEM slope mapping and analysis
35 DTMs [9-11], Gullied, Adjacent, Non-Gullied

Formation Mechanism Matrix
Liquid, dry & sublimation processes

3. Results

→287/1558 surveyed HiRISE images contained equatorial gullies.

→*Statistically significant spatial clustering* – equatorial gullies are **non-randomly distributed** (Fig 3.).

→Gullied footprints are associated with **higher thermal inertia** terrain, pointing to **rocky, bedrock-exposed areas**.

→Notable *exception* in Amazonis Planitia in low-TI terrain.

→Rockiness alone does not fully explain their occurrence.

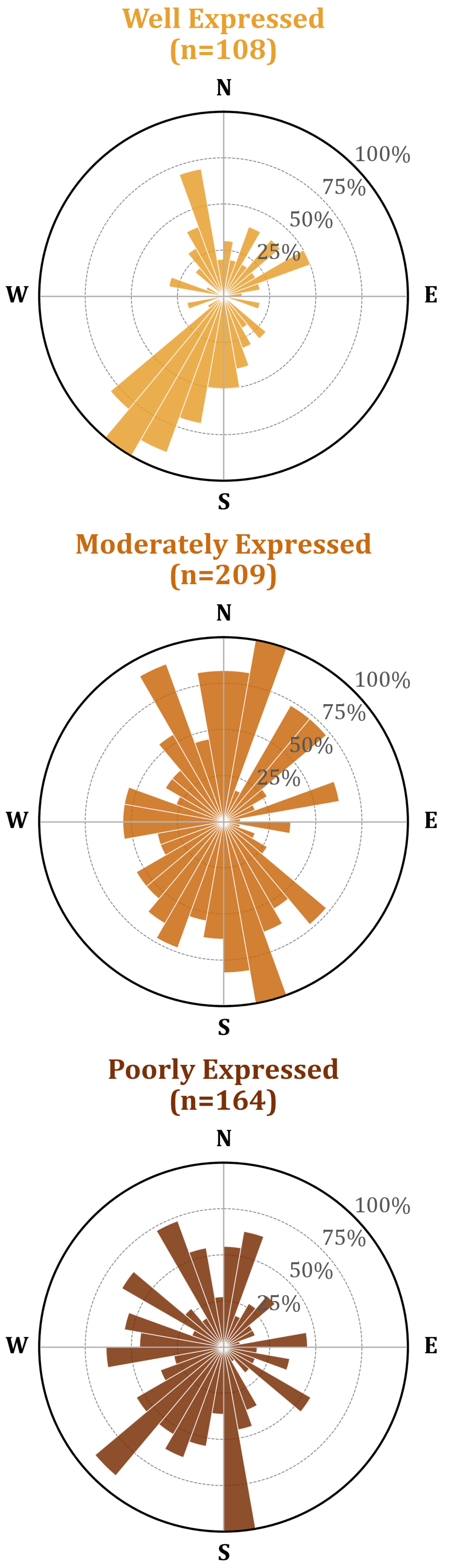

Figure 2. *Orientation of equatorial gullies across the full 25°N-25°S band by channel expression (well/moderate/poor).*

→**No global orientation preference** (Fig 2.), which is inconsistent with present-day aspect dependent frost processes [3, 12, 13].

→The **SW-signal in well-expressed gullies** is for the majority a signal from the **Southern Hemisphere**.

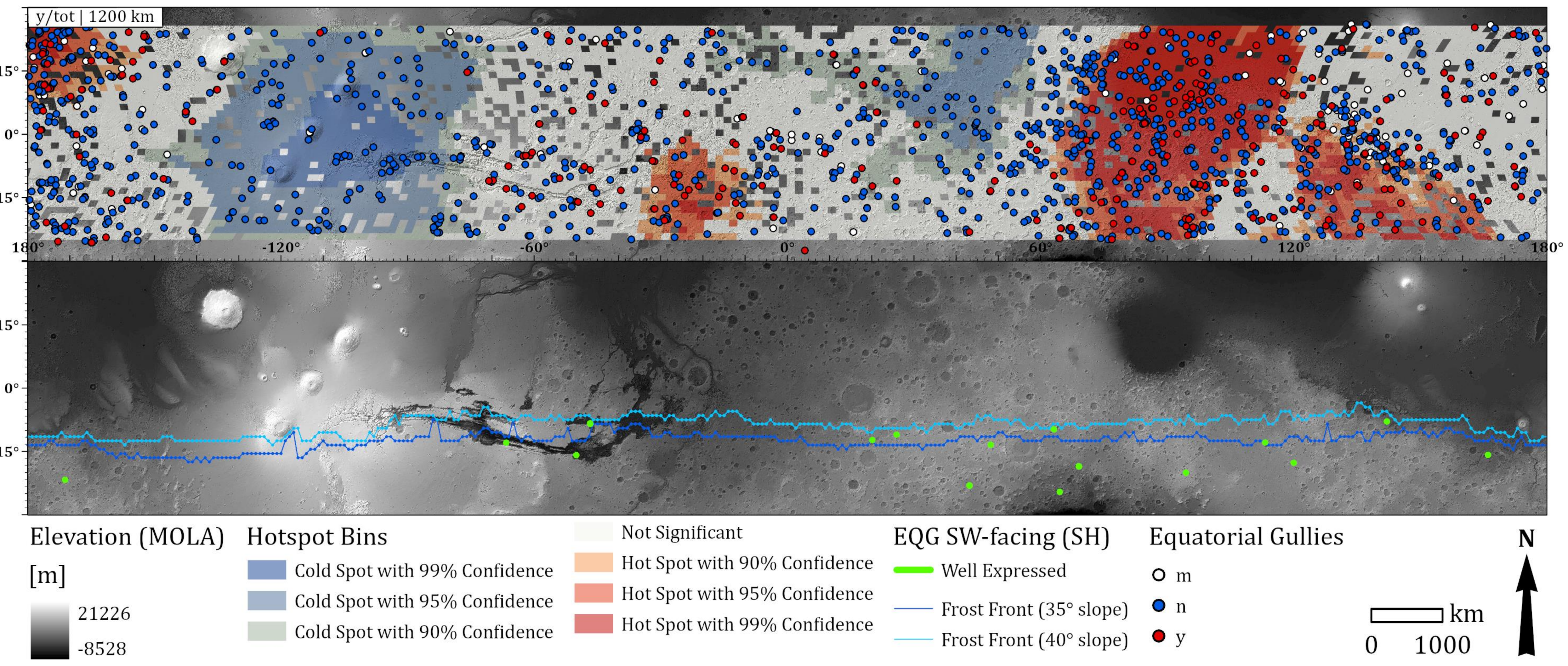

Figure 3. *(Top) Regional (1200 km) hot spot analysis of equatorial gully locations normalized by HiRISE imagery availability. (Bottom) Well-expressed, SW-facing gullies in the southern hemisphere, all fall poleward of modelled H_2O-frost stability boundaries for steep (35°/40°) south-facing slopes [14].*

→The SW-facing signal overlaid against **modelled H_2O frost stability lines for steep, south-facing slopes** [14] shows all 34 gullied sites sit poleward of the modelled frost boundaries (Fig. 3).

→This relates the orientation of a subset of EQG to **H_2O sublimation** as a potential *volatile formation mechanism*.

→The remainder may represent a different or older process, potentially showcasing **relict features** from a higher-obliquity in the past.

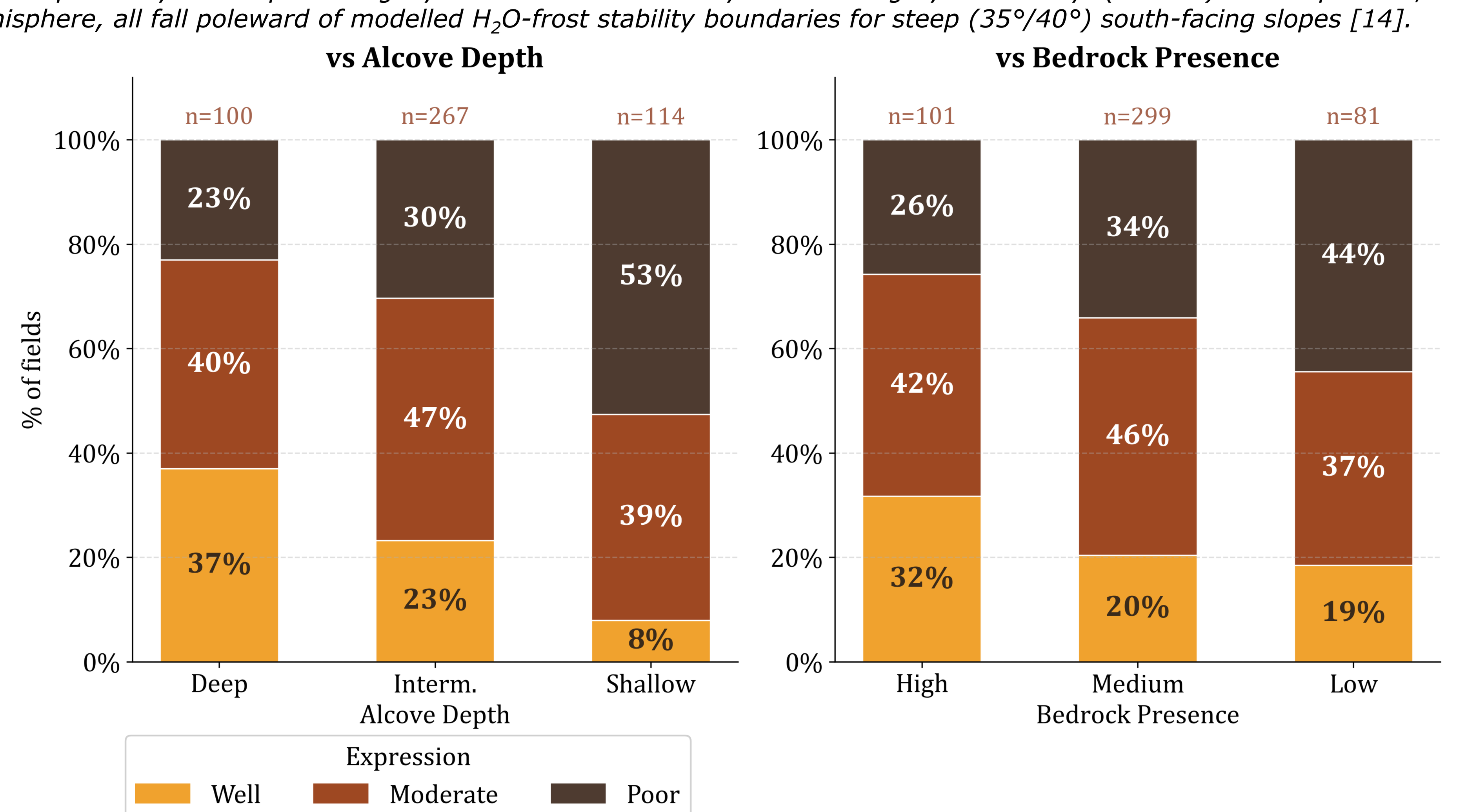

Figure 4. *Well-expressed equatorial gullies correlate with higher bedrock exposure and deeper bedrock alcoves. Decreasing for poorly expressed gullies. Bedrock exposure and alcove depth co-vary directly. Suggesting that morphological development/expression is impacted by the availability of exposed bedrock.*

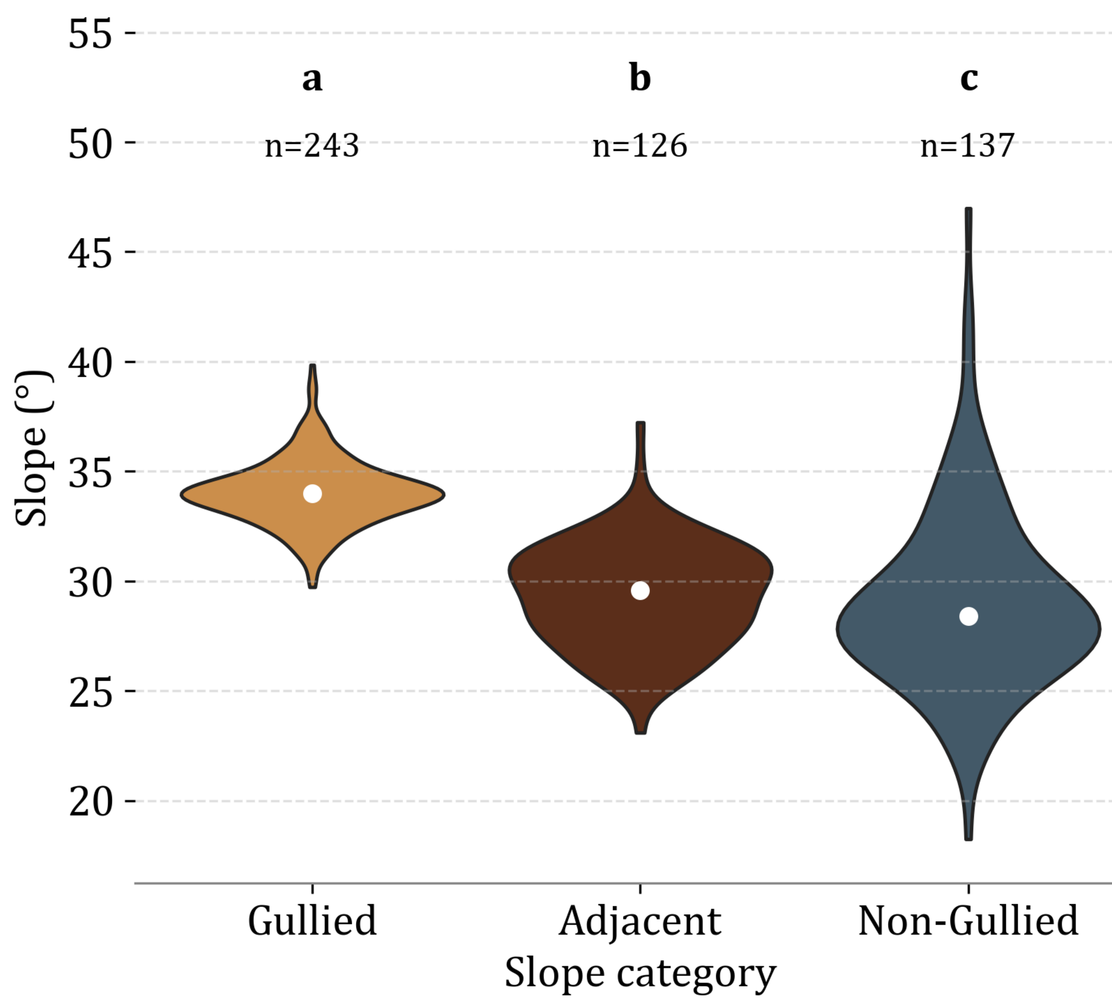

Figure 5. *Gullied slopes (median 33.9°) are significantly steeper than adjacent (29.6°) and non-gullied (28.4°) slopes, although the tails overlap considerably.*

→**Gullied slope angles** cluster tightly around 30-40° (near angle of repose) (Fig. 5).

→**Non-gullied and adjacent slope angles** span a wider range with lower medians.

→All three categories are significantly distinct, implying **steep slopes are necessary** for EQG formation, **but not sufficient on their own**.

→*Plenty of steep slopes have no equatorial gullies.*

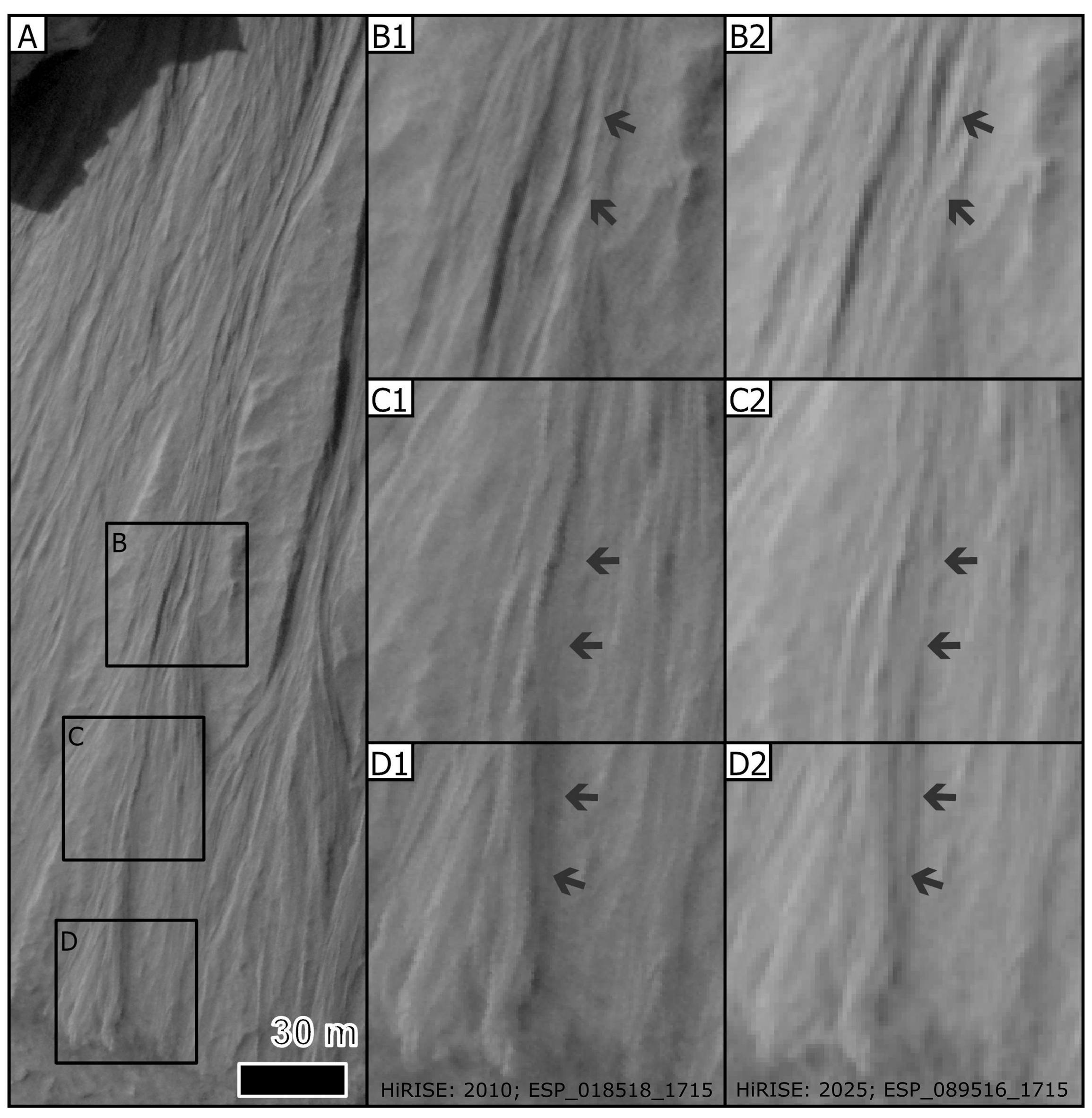

→**Present day activity** observed in equatorial gullies [6] (Fig. 6).

→Example location in Ganges Chasma with signs of **erosion and deposition** along a channel between two acquisition dates.

→At least some equatorial gullies show signs of **active morphological change under present-day Martian conditions**.

Figure 6. *Morphological changes along an equatorial gully channel in Ganges Chasma. Arrows indicate the locations of erosion and deposition.*

Formation Mechanism

→*Liquid water and seasonal CO_2-frost are ruled out* as formation mechanisms by present day conditions.

→*Dry processes* are insufficient on their own to form the full morphology.

→**H_2O-frost sublimation is the best supported present-day mechanism.**

→*With the broader population possible containing relict features from a higher obliquity past.*

4. Conclusions

→First systematic survey of equatorial gullies (25°N-25°S), identifying **287 gullied HiRISE footprints with a non-random distribution and strong regional clustering**.

→**Rocky, high thermal inertia terrain** is dominant but not exclusive.

→**No global orientation preference** – inconsistent with present-day frost.

→SW-facing subset on the southern hemisphere within modelled boundaries **suggestive of H_2O-frost involvement**.

→Steep slopes (30°-40°) necessary but not sufficient on their own.

→**H_2O-frost sublimation is the most plausible present-day mechanism.**

5. References
[1] Harrison et al. (2015) Icarus, https://doi.org/10.1016/j.icarus.2015.01.022.
[2] Malin et al. (2007) JGR: Planets, https://doi.org/10.1029/2006JE002808.
[3] Noblet et al. (2024) Icarus, https://doi.org/10.1016/j.icarus.2024.116147.
[4] Auld & Dixon (2016) Planetary and Space Science, https://doi.org/10.1016/j.pss.2016.08.002.
[5] McEwen et al. (2018) European planetary science congress.
[6] Thomas et al. (2020) Icarus, https://doi.org/10.1016/j.icarus.2019.113566.
[7] Vincendon (2015) JGR: Planets, https://doi.org/10.1002/2015JE004909.
[8] Viola & McEwen (2018) JGR: Planets, https://doi.org/10.1002/2017JE005366.
[9] Beyer et al. (2018) Earth and Space Science, https://doi.org/10.1029/2018EA000409.
[10] Sutton et al. (2022) Remote Sensing, https://doi.org/10.3390/rs14102403.
[11] Quantin-Nataf et al. (2018) Planetary and Space Science, https://doi.org/10.1016/j.pss.2017.09.014.
[12] Conway et al. (2017) Geological Society, London, Special Publications, https://doi.org/10.1144/SP467.3.
[13] Heldmann et al. (2005) JGR: Planets, https://doi.org/10.1029/2004JE002261.
[14] Lange et al. (2023) JGR: Planets, https://doi.org/10.1029/2023JE007915.